Journal of Ethnopharmacology 317 (2023) 116770

Contents lists available at ScienceDirect

Journal of Ethnopharmacology

journal homepage: www.elsevier.com/locate/jethpharm

# The antihyperuricemia activity of Astragali Radix through regulating the expression of uric acid transporters via PI3K/Akt signalling pathway

Meng-Qi Zhang [a,1], Ke-Xin Sun [b,1], Xu Guo [a], Ying-Ying Chen [a], Cai-Yun Feng [a], Jia-Shu Chen [a], Joao C.M. Barreira [c], Miguel A. Prieto [d], Jin-Yue Sun [a,*], Jian-Dong Zhang [e,**], Ning-Yang Li [f,***], Chao Liu [a,****]

[a] Key Laboratory of Novel Food Resources Processing, Ministry of Agriculture and Rural Affairs/Key Laboratory of Agro-Products Processing Technology of Shandong Province, Institute of Agro-Food Science and Technology, Shandong Academy of Agricultural Sciences, 23788 Gongye North Road, Jinan, 250100, PR China
[b] Key Laboratory of Food Processing Technology and Quality Control in Shandong Province, College of Food Science and Engineering, Shandong Agricultural University, Taian, 271018, PR China
[c] Centro de Investigação de Montanha (CIMO), Instituto Politécnico de Bragança, Campus de Santa Apolónia, 5300-253, Bragança, Portugal
[d] Universidade de Vigo, Nutrition and Bromatology Group, Department of Analytical Chemistry and Food Science, Faculty of Science, E32004, Ourense, Spain
[e] Department of Oncology, The First Affiliated Hospital of Shandong First Medical University & Shandong Provincial Qianfoshan Hospital, Shandong Key Laboratory of Rheumatic Disease and Translational Medicine, Jinan, 250014, PR China
[f] College of Food Science and Engineering, Ocean University of China, Qingdao, 266003, PR China

ARTICLE INFO

Handling Editor: Dr. Thomas Efferth

*Keywords:*
Astragali Radix
Hyperuricemia
UA Transporter
Mechanism

ABSTRACT

*Ethnopharmacological relevance:* Astragali Radix (AR) is the dry root of the leguminous plants *Astragalus membranaceus* (Fisch) Beg. var. *mongholicus* (Beg) Hsiao, and *Astragalus membranaceus* (Fisch) Bge., being used as a medicinal and edible resource. AR is used in traditional Chinese medicine prescriptions to treat hyperuricemia, but this particular effect is rarely reported, and the associated mechanism of action is still need to be elucidated.
*Aim of the study:* To research the uric acid (UA)-lowering activity and mechanism of AR and the representative compounds through the constructed hyperuricemia mouse and cellular models.
*Materials and methods:* In our study, the chemical profile of AR was analysed by UHPLC-QE-MS, as well as the mechanism of action of AR and the representative compounds on hyperuricemia was studied through the constructed hyperuricemia mouse and cellular models.
*Results:* The main compounds in AR were terpenoids, flavonoids and alkaloids. Mice group treated with the highest AR dosage showed significantly lower ($p < 0.0001$) serum uric acid (208 ± 9 μmol/L) than the control group (317 ± 11 μmol/L). Furthermore, UA increased in a dose-dependence manner in urine and faeces. Serum creatinine and blood urea nitrogen standards, as well as xanthine oxidase in mice liver, decreased ($p < 0.05$) in all cases, indicating that AR could relieve acute hyperuricemia. UA reabsorption protein (URAT1 and GLUT9) was down-regulated in AR administration groups, while the secretory protein (ABCG2) was up-regulated, indicating that AR could promote the excretion of UA by regulating UA transporters via PI3K/Akt signalling pathway.
*Conclusion:* This study validated the activity, and revealed the mechanism of AR in reducing UA, which provided experimental and clinical basis for the treatment of hyperuricemia with it.

* Corresponding author.
** Corresponding author.
*** Corresponding author.
**** Corresponding author.
*E-mail addresses:* moon_s731@hotmail.com (J.-Y. Sun), zhangjd165@sina.com (J.-D. Zhang), ningyangli@126.com (N.-Y. Li), liuchao555@126.com (C. Liu).
[1] These authors contributed equally to this work.

https://doi.org/10.1016/j.jep.2023.116770
Received 27 April 2023; Received in revised form 6 June 2023; Accepted 9 June 2023
Available online 10 June 2023

## 1. Introduction

Hyperuricemia is the second largest metabolic disease (being surpassed only by diabetes), being characterized as a disorder of purine nucleosides metabolism, and its incidence has been increasing year by year (Lin et al., 2019; Dalbeth et al., 2018). At present, the main ways to reduce physiologic uric acid (UA) include inhibition of UA production and stimulating UA excretion. Xanthine oxidase (XOD) is the most important biological protease that regulates the production of UA, acting as the rate-limiting enzyme in the nucleoside and purine metabolic pathways (Liu et al., 2010; Zeng et al., 2019). In what concerns its excretion, UA enters the renal tubule after being filtered by the glomerulus, and is reabsorbed into the blood by uric acid transporter 1 (URAT1) or glucose transporter 9 (GLUT9) in the proximal tubule; afterwards, UA passes through adenosine triphosphate transporter G2 (ABCG2) and is finally secreted into the urine (Diaz et al., 2015; Kaito et al., 2013).

Traditional Chinese medicine is quite effective in the treatment of hyperuricemia (Song et al., 2021; Zhou and Chen, 2014; Yong et al., 2018; Han et al., 2020). Astragali Radix (AR) is the dry root of the leguminous plants *Astragalus membranaceus* (Fisch) Beg. var. *mongholicus* (Beg) Hsiao, and *A. membranaceus* (Fisch) Bge., being used as a medicinal and edible resource. AR is the representative of Qi-benefiting traditional Chinese medicine, having validated effects on diuresis, detumescence, promoting body fluid, or nourishing blood, among others (Chinese Pharmacopoeia Commission, 2020; Zheng et al., 2020). AR contains a variety of chemical constituents, including triterpene saponins, flavonoid and polysaccharide compounds (Bian et al., 2008; Hong et al., 2016; Yuan et al., 2019; Jin et al., 2014). Modern pharmacology confirmed that AR has diuretic, renal protection, or body immunity enhancement, besides a few other effects (Bin et al., 2020; Zhang et al., 2007). AR is also used in traditional Chinese medicine prescriptions to treat hyperuricemia (Wang et al., 2020; H. Liu et al., 2017; Zhang et al., 2018), but this particular effect is rarely reported, and the associated mechanism of action is still need to be elucidated (Wang et al., 2021).

Hence, the chemical profile of AR was analysed by UHPLC-QE-MS and the activity of the detected compounds on hyperuricemia was evaluated in cellular and mouse models. The mechanism of action supporting the investigated anti-hyperuricemia effect was studied by Western-Blot, aiming providing a scientific basis for AR activity against hyperuricemia.

## 2. Materials and methods

### 2.1. Chemicals and reagents

UA, adenine alcohol, potassium oxazine, allopurinol, astragaloside IV (As), calycosin-7-glucoside (Ca) and AKT inhibitor VIII were purchased from Macklin Biochemical Co. Ltd. (Shanghai, China); Tween-20, 20 × TBS, glycine, Tris-base, Sodium dodecyl sulphate (SDS), and 5x Triglycine electrophoretic buffer were acquired from Beijing Solarbio Science & Technology Co., Ltd. (Beijing, China); ponceau staining solution, SDS-PAGE protein buffer (5x), RIPA lysis solution, and protease inhibitor MSF were provided by Beyotime Science & Technology Co., Ltd. (Shanghai, China). The test kits for UA, XOD, creatinine, urea nitrogen, alanine transaminase (ALT), and aspartate transaminase (AST) were purchased from Jiancheng Biotechnology (Nanjing, China); ABCG2, GLUT9 and URAT1 polyclonal antibody, Goat Anti-Mouse IgG (H + L), and Goat Anti-Rabbit IgG (H + L) were obtained from Proteintech Group (USA); GAPDH Monoclonal Antibody was furnished by Wuhan Servicebio Technology Co., Ltd. (Wuhan, China).

### 2.2. AR materials, and UHPLC-QE-MS analysis of AR

AR (*A. membranaceus* (Fisch) Bge., voucher specimen No. 20210908) used in this trial was purchased from Jianlian Traditional Chinese Medicine Shop, Jinan, China, and stored at Key Laboratory of Agro-Products Processing Technology of Shandong Province, Jinan, China. The conventional method, heat-reflux extraction was used to obtain the experiment sample (Tang et al., 2009). After drying, AR was powdered, soaked for 1 h (100 g of powder in 1000 mL of distilled water), and then heated and reflowed for 2 h at 100 °C. The residue was reflowed again in distilled water (800 mL) for 2 h. The filter liquor was combined and concentrated with rotavapor at 40 °C to obtain the water sample of AR.

A UHPLC system (Agilent, 1290) coupled to a Q Exactive Focus mass spectrometer (QE-MS/MS) was used to obtain the chemical profiles of AR. The analytical solvents were water (solvent A) and acetonitrile (solvent B), both containing 0.1% formic acid. The elution gradient was employed as follows: 0–6 min, 5–30% B; 6–6.5 min, 30% B; 6.5–12 min, 30–70% B; 12–12.5 min, 70% B; 12.5–18 min, 70–100% B; 18–25 min, 100% B; 25–26 min, 100-5% B; 26–30 min, 5% B. The flow was 0.4 mL/min, and the injection volume was 5 μL. A Waters UPLC BEH $C_{18}$ column (1.7 μm, 2.1*100 mm) was used for compound separation.

MS and MS/MS data were gathered by an Xcalibur software at IDA acquisition mode. The source parameters were, turbo spray: 400 °C; ion spray voltage: −3600 V (negative ion mode)/4000 V (positive ion mode); sheath gas flow: 45 Arb; aux gas flow: 15 Arb; collision energy: 15/30/45 in NCE mode. The original off-machine data (.raw) files were added to the Progenesis QI software for retention time screening, peak identification and extraction, and other parameters. The molecular ion peaks and fragment ions were used to obtain the molecular formulas by comparing with a traditional Chinese medicine database.

### 2.3. Effects of AR on acute hyperuricemia mice

#### 2.3.1. Animals and treatment

Kunming mice (n = 80, male, weight 20 ± 2 g) were supplied by Jinan Pengyue Experimental Animal Centre, Jinan, China (NO. SCXK [Henan] 2021-0007). One week before the laboratorial test, mice were fed *ad libitum*, under the following conditions: temperature 25 ± 2 °C, dampness 50–60%, and alternate light/dark for 12 h each.

Mice were allocated randomly into seven groups (n = 10): normal control group; positive control group (allopurinol); model control group (potassium oxonate and adenine treated); three AR groups: low-dosage AR group (ARL), medium-dosage AR group (ARM), high-dosage AR group (ARH), and combination group (ARM-allopurinol). The established hyperuricemia model mice were carried out as previously reported, mice in the normal control group were given 0.5% sodium carboxymethyl cellulose (CMC-Na), 10 mL/kg. Mice in the remaining groups were administrated with 200 mg/kg adenine, and 500 mg/kg potassium oxonate (both dissolved in CMC-Na and given 10 mL/kg) once daily for two weeks (Umekawa et al., 2003). Two weeks later, mice in the ARL, ARM and ARH groups were given AR at 130 mg/kg/d, 260 mg/kg/d, and 520 mg/kg/d, respectively. Mice in the positive control group were given an allopurinol aqueous solution (10 mg/kg/d), and the mice in the combination group were given a mixed solution of allopurinol and medium-dose AR (10 mg/kg/d + 260 mg/kg/d). All mice were dosed by intragastric administration once a day for 14 days.

After 1 h of administration on the 13th day, all mice in each group were placed in sterile and clean mouse cages, and after natural defecation, the excreted faeces were collected with sterile forceps and placed in a 1.5 mL sterile EP tube. The tweezers were sterilized for the next sampling until all mouse faeces were collected. The samples were store in −80 °C refrigerator immediately until use. On the 14th day, all mice were fasted immediately after the last administration, and drunk water freely. One hour after the last gavage, the head and neck of the mice were grasped, the tail was lifted, and the lower abdomen of the mice was gently pressed with fingers. After the mice urinated, the urine was drawn into a sterile EP tube with a syringe. The urine supernatant was obtained after centrifuging at 3000 rpm for 10 min and stored at −20 °C for later use. After 8 h, mice were anesthetized (the orbital blood was collected and centrifuged at 3000 rpm for 10 min), and then sacrificed. The kidney

and liver samples were excised, and kept at −80 °C until analysis.

### 2.3.2. The UA, serum creatinine (SCr), and blood urea nitrogen (BUN) levels in mice

Before testing, urine was diluted ten times with normal saline. Faeces were mixed with normal saline (1 g:9 mL), homogenized for 60 s, and centrifuged at 10000 rpm (10 min). The UA levels in serum, urine and faeces were determined by phosphotungstic acid reduction method, SCr levels were tested by sarcosine oxidase approach, and BUN levels were evaluated by urease methodology. The detection steps were performed strictly following the instruction steps in the kit. The corresponding level of each indicator was calculated according to the absorbance obtained using a microplate reader, and the instruction formula.

### 2.3.3. XOD, ALT and AST activities in mice

XOD catalyses the conversion of hypoxanthine to xanthine, in which $O^{2-}$ radicals meet the electron acceptor and chromogenic agent to form a purplish red complex; the activity of XOD can be inferred from the amount of violet red complex produced. ALT and AST are two indicators used to assess the body's liver function or the extent of liver damage. The specific reagent composition, preparation, steps and calculation formula are carried out according to the steps indicated in the kit instructions.

### 2.3.4. Histopathological analyses

The histopathological analyses were performed according to previous reports (Zhang et al., 2020; Chen et al., 2022). The liver tissues were fixed by stationary liquid for 3 d, embedded in paraffin, cut into 4 μm thick sections, and stained with H&E. Cell features and liver section was recorded by an optical microscope (NIKON Eclipse, Japan) at 200× magnification, followed by detailed pathological analysis. The histopathological experiments of kidney was the same as those performed in liver tissue. The histopathological scoring of liver and kidney was expressed as the obtained average in grades of 0 (normal), 1 (mild change), 2 (mild to moderate severity), 3 (moderate severity) and 4 (serious severity) (Mann, 2019).

### 2.3.5. Effect of AR on the expression of UA transporters

UA transporters expression was examined using western blotting analysis and following our previous experiment (Chen et al., 2022). Kidney and intestine tissues protein was collected in lysis buffer (added with protease inhibitor), and protein concentration was quantified using the bicinchoninic acid assay (BCA) kit. Proteins (50 μg) were separated on 10% SDS-PAGE, and, after electrophoresis, transferred to polyvinylidene fluoride (PVDF) membranes by Bio-Rad transblot system. The membranes were blocked with 5% non-fat milk (1.5 h; room temperature). Then, the membranes were hatched with ABCG2, GLUT9, URAT1 and GAPDH antibodies overnight at 4 °C, washed with TBST, and incubated for 2 h with the corresponding secondary antibodies at 37 °C. Membranes were further tested with a ChemiDoc imaging system equipped with Image Lab 5.1. software (BioRad Laboratories Inc., America).

## 2.4. Effects of AR on hyperuricemic cell models

Human colon carcinoma cell line (CACO-2), and human renal tubular epithelial cell line (HK-2) were purchased from the Peking Union Medical College (Beijing, China). Cell cultures were kept in Dulbecco's Modified Eagle Medium (DMEM), supplemented with 5% foetal bovine serum (FBS), 100 U/mL penicillin and 100 mg/mL streptomycin in a 5% $CO_2$ incubator at 37 °C.

The effects of different UA and AR dosages on the survival rate of both cell lines were evaluated. Results showed that when the concentration of UA reached 1250 μg/mL, cell survival rate decreased significantly, indicating that concentrations of UA higher than 1250 μg/mL could produce some toxicity to CACO-2 and HK-2 cells (Fig. 1A). Therefore, the 1000 μg/mL UA concentration was selected to build the hyperuricemic cell model. The following groups were tested: i) normal control group, ii) model control group, iii-v) AR treated groups (0.5, 1, and 2 mg/mL), vi-vii) astragaloside IV (As) (20, 40 μg/mL) treated group and viii-ix) calycosin-7-glucoside (Ca) (20, 40 μg/mL) treated group (Fig. 1B).

After the cells in each group were incubated with different drugs for

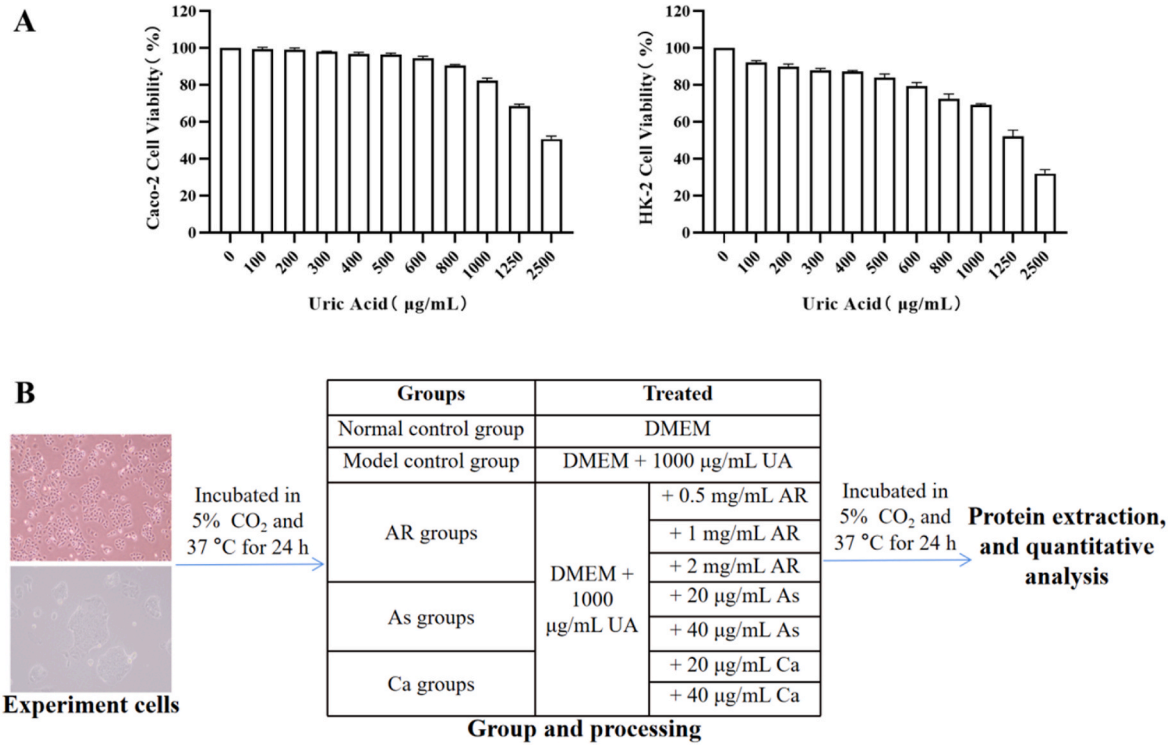


**Fig. 1.** Effect of UA on cell viability of Caco-2 and HK-2 cells (A), and the grouping and treatment in each group in this experiment (B).

24 h, the medium was discarded, washed three times with 1 mL of pre-cooled PBS, and further added with 200 μL of PBS. Cell samples were obtained by centrifugating 12,000 rpm for 10 min at 4 °C. The western blotting analysis of cells were the same as that used for kidney samples.

### 2.5. Molecular docking experiments of astragaloside IV and calycosin-7-glucoside

As and Ca are the main quality control components of AR in Chinese Pharmacopoeia Commission (Chinese Pharmacopoeia Commission, 2020). In cellular experiments, they showed certain activity to regulate the UA transporters, so molecular docking were used to investigate their binding mode and activity to the transporters. The protein models of ABCG2, GLUT9 and URAT1 (A4HSQ1, Q3T9X0 and Q3ZAV1) were acquired from AlphaFold2 Protein Structure Database (https://alphafold.ebi.ac.uk/). Proteins were hydrogenated and Gasteiger charges were calculated with AutoDock Tools 1.5.6 software and saved as pdbqt files. The 2D structures of small molecule compounds were download from PubChem (https://pubchem.ncbi.nlm.nih.gov/), and the energy was minimized with ChemBio3D. The compounds atomic charges were added, atom types were assigned, and rotation centres were selected with AutoDock Tools 1.5.6 software. All flexible bonds were rotatable by default and saved in pdbqt format as docking ligands. A Grid box was set to wrap the transport region, and AutoDock Vina was used for semi-flexible docking with exhaustiveness at 24. Finally, the conformation with the highest scoring value was selected to analyse the results with Discovery Studio Visualizer 2019, and PyMOL was used for mapping.

### 2.6. Statistical analysis

Statistical analyses were performed using GraphPad Prism 7.0, and data were presented as mean ± standard deviation (SD). Significant differences between groups were measured by Student's t-test. All statistical analyses were performed at $p < 0.05$ level of significance.

## 3. Results and discussion

### 3.1. Chemical profile of AR

The chemical profile of AR was obtained through UHPLC-QE-MS (Fig. 2A), and 348 compounds were identified, including 98 terpenoids, 50 flavonoids, 36 alkaloids, 29 phenylpropanoids, 19 amino acid derivatives, among other less abundant groups, which is the same as previous results (Yuan et al., 2019; Jin et al., 2014). The formula, theoretical mass, error, etc., of identified compounds were shown in Table S1. The previous reports indicated that various bioactive compounds (alkaloids, flavonoids, triterpenoids) had potential anti-hyperuricemia activities (Syahrina et al., 2020; Liu et al., 2010). The relative content of alkaloids was most with 27.63% with the primary compounds, erucamide (the relative content of 8.80%), guanine (4.38%), adenosine (3.00%), guanosine (2.95%), and pipecolic acid (2.95%). The relative content of amino acid derivatives was 21.61%, with master components of arginine (11.15%), L-isoleucine (5.28%), and L-tryptophan (2.80%). The relative content of flavonoids was 14.85% with the major ononin (7.90%), and biochanin-7-O-glucoside (2.00%). The terpenoids were the most abundant compounds with representative astragaloside II (the relative content of 0.76%), and astragaloside IV (0.37%). The astragalosides, i.e. astragaloside I-IV, belong to cycloartane-type triterpenoids. And they are considered as the main ingredients with good pharmacological activities of AR (Yan et al., 2010; Zhang et al., 2007).

The mass spectra, speculative fragments, and structures of the representative components, astragaloside II-IV and isomucronulatol-7-O-glucoside, were shown in Fig. 2B. The peaks of precursor and product of astragaloside IV were $m/z$ 785.47 → 143.11, which was the same as previous reports (Yan et al., 2010). The peaks of precursor and product of astragaloside III were $m/z$ 783.45 → 489.37 appearing typical cycloartane daughter ion. The peaks of precursor and product of isomucronulatol-7-O-glucoside were $m/z$ 465.17 → 303.12, and 465.17 → 163.17 indicating flavonoid nuclei, and dehydrated glucose, respectively.

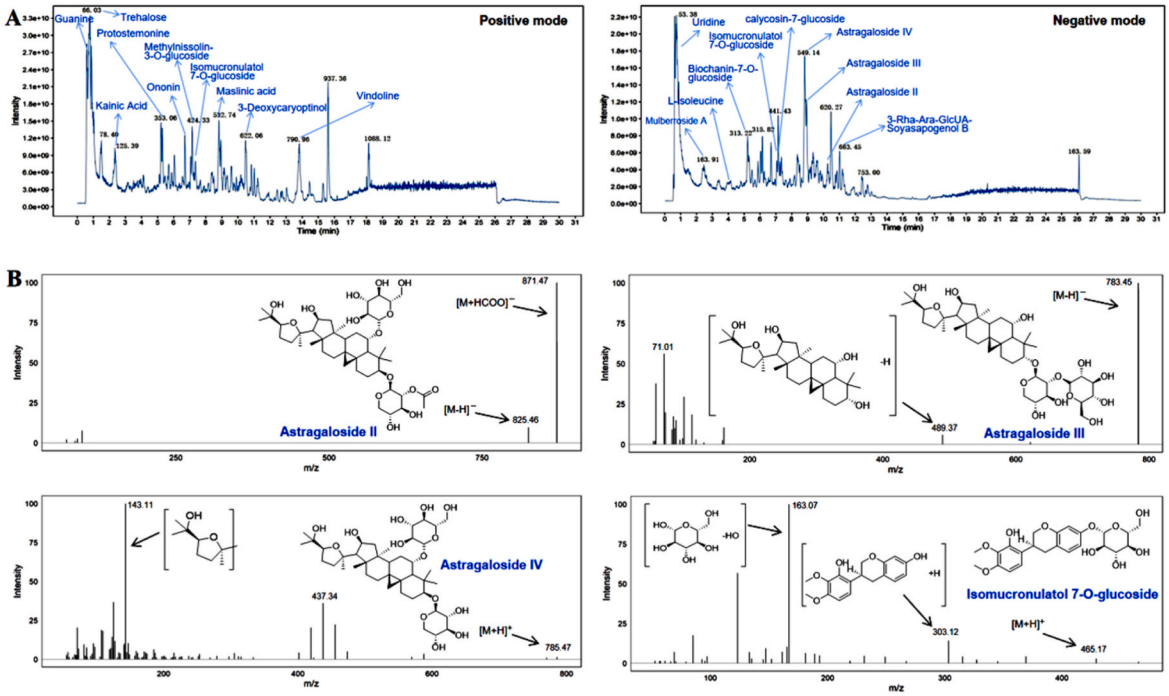


**Fig. 2.** The total ion chromatography of AR in positive and negative modes (A), and the mass spectrogram of representative compounds in AR (B).

### 3.2. Effects of AR on acute hyperuricemia mice

#### 3.2.1. Effects of AR on UA levels in mice serum, urine and faeces

Hyperuricemia is caused by increased UA synthesis or poor UA excretion. Therefore, the modeling methods of hyperuricemia mostly rely on supplementing high purine substances or inhibiting the activity of enzymes related to UA excretion. In this study, mice were administered with potassium oxonate and adenine to establish a hyperuricemia mouse model. Potassium oxonate is a uricase inhibitor, which can inhibit uricase to catalyse UA into allantoin. Adenine is a substrate for UA synthesis and can increase the synthesis of UA. Potassium oxonate and adenine can stimulate UA expression in mice by inhibiting the decomposition and increasing the synthesis of UA, functioning as a hyperuricemic model (Wang et al., 2010). Although UA is primarily excreted through the kidneys in the form of urine, patients with kidney failure experience an increase in intestinal UA excretion to compensate the decrease in renal excretion (Ichida et al., 2012).

In order to evaluate the effect of AR on UA metabolism *in vivo*, this compound was quantified in mouse serum, urine and faeces. As shown in Table 1, after the modelling of potassium oxonate and adenine, the level of serum UA (SUA) in the model control group (317 ± 11 μmol/L) was significantly higher ($p < 0.0001$) than the one quantified in the normal control group (208 ± 9 μmol/L), revealing that the hyperuricemia model was successful. In comparison with the model control group, the levels of SUA in groups administrated with AR were significantly decreased ($p < 0.01$), following a dose-dependent correlation. The SUA levels in high-dose AR group and ARM-allopurinol group (with 212 ± 23 and 208 ± 15 μmol/L, respectively) were close to that in the normal control group ($p < 0.0001$). Compared with the model control group, the levels of UA in urine (UUA) and faeces (FUA) in the AR group (1845 ± 18 and 6320 ± 53 μmol/L, respectively) were also raised in a dose-dependent manner (Table 1). These results indicated that AR could lower the UA level in the hyperuricemia mice, due to the fact that AR promoted the excretion of UA through urine and faeces.

#### 3.2.2. Effect of AR on XOD activity in hyperuricemic mice

Purine is oxidized by XOD to hypoxanthine and finally to UA (Hille et al., 2006). XOD is the most important biological protease regulating the production of UA in purine metabolism. If the expression or activity of XOD is raised, the production of UA increases (Zeng et al., 2019). As shown in Fig. 3, the liver XOD activity in the model control group mice was remarkably higher than that measured in normal control group ($p < 0.01$). In addition, the liver XOD activity of mice administrated with AR group decreased in a dose-dependent manner. Especially, the XOD activities in high-dose AR group and ARM-allopurinol group were decreased remarkably compared with the model control group ($p < 0.05$). The experimental results showed that AR could reduce the activity of XOD in the liver of hyperuricemic mice to decrease the production of UA, thereby alleviating the hyperuricemia led by potassium oxonate and adenine modelling.

**Table 1**
Effects of AR on SUA, UUA and FUA levels in mice.

| Groups | Treatment (mg/kg/d) | SUA (μmol/L) | UUA (μmol/L) | FUA (μmol/g) |
|---|---|---|---|---|
| Normal | – | 208 ± 9 | 2066 ± 12 | 6121 ± 66 |
| Model | – | 317 ± 11$^{\#\#\#\#}$ | 1845 ± 18$^{\#\#\#\#}$ | 6320 ± 53 |
| Allopurinol | 10 | 221 ± 16**** | 1969 ± 6** | 6550 ± 35 |
| ARL | 130 | 254 ± 27** | 1890 ± 9 | 6656 ± 35 |
| ARM | 260 | 232 ± 19*** | 1933 ± 10* | 7205 ± 88** |
| ARH | 520 | 212 ± 23**** | 2036 ± 6*** | 7488 ± 159** |
| ARM + Allopurinol | 260 + 10 | 208 ± 15**** | 1994 ± 23** | 6957 ± 265* |

**Note:** $^{\#\#\#\#}$ indicates a significantly different level from that of normal control group, $p < 0.0001$; *, **, ***, ****indicate a significantly different level from that of model control group at $p < 0.05$, $p < 0.01$, $p < 0.001$, and $p < 0.0001$, respectively.

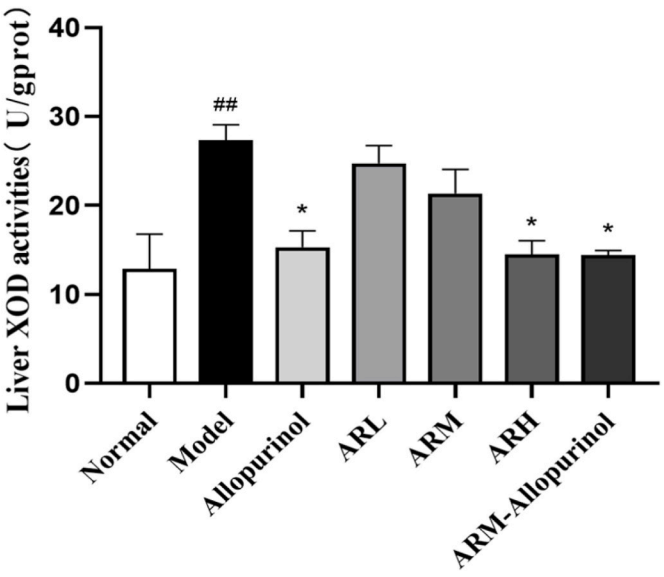


**Fig. 3.** Effect of AR on XOD activity in the mouse liver. Note: $^{\#\#}$ indicated a significantly different level from that of normal control group at $p < 0.01$; * indicated a significantly different level from that of model control group at $p < 0.05$.

#### 3.2.3. Effect of AR on renal injury in hyperuricemic mice

Serum creatinine (SCr) and blood urea nitrogen (BUN) are vital indicators for clinical diagnosis of renal function, and their elevations indicate impaired renal function and problems with UA excretion (Xu et al., 2020; Chen et al., 2022). In our study, the model control group had higher levels of SCr and BUN than the normal control group (Fig. 4A, $p < 0.01$), indicating that the administration of the modelling drug caused kidney damage in mice. After AR intervention, the levels of SCr and BUN in hyperuricemic mice were significantly reduced, and the high-dose AR group had stronger activity than the positive drug group ($p < 0.05$). It was worth noting that the combined use of AR and allopurinol brought the levels of SCr and BUN lower than that in model control group ($p < 0.01$), but closer to the normal control group. The above results illustrated that AR had obvious protective effect on mice kidney function and could alleviate the renal injury in hyperuricemia mice.

Pathological section is an intuitive and important indicator for evaluating the condition of tissues (Wang, 2016). Histopathological sections can evaluate intuitively the effect of AR on renal injury of hyperuricemia mice. The renal tissue of the normal control group showed regular renal structure with normal glomerulus structure, well appeared renal cells, and clear renal tubule structure (Fig. 4B). However, in the hyperuricemia group, acidophilia of epithelium cytoplasm attenuated (black arrow), a small amount of renal tubule expand, renal tubular epithelial cells flattened (orange arrow), necrotic cell debris appeared in the lumen of the renal tubules (red arrow), glomerular capillary congested (green arrow), and a small perivascular lymphocyte infiltrated (blue arrow). Compared with model control group, the AR administrated groups effectively improved renal injury, and the improvement effect was remarkably better than that of positive control group, as verified by histopathological scoring (Fig. 4C).

#### 3.2.4. Effects of AR on liver function in hyperuricemia mice

XOD is an important enzyme for the physiological production of UA, which exists mainly in the liver (Fukunari et al., 2004; Zeng et al., 2019).

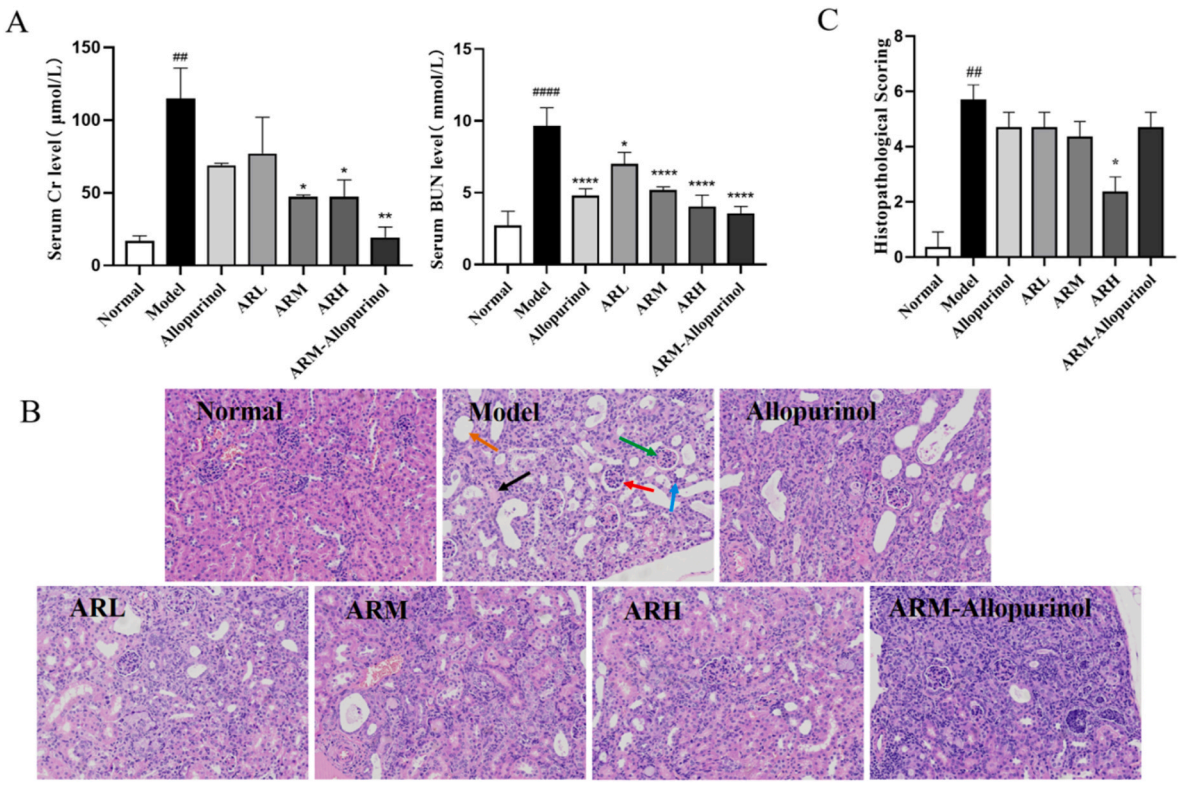


**Fig. 4.** Effect of AR on renal injury in hyperuricemic mice. Note: SCr and BUN levels in mice kidneys (A), pathological section of kidney tissue (B), and the score of pathological section. $^{\#\#}$, $^{\#\#\#\#}$ indicated a significantly different level from that of normal control group at $p < 0.01$, $p < 0.0001$, respectively; *, **, ****indicated a significantly different level from that of model control group at $p < 0.05$, $p < 01$, and $p < 0.0001$, respectively.

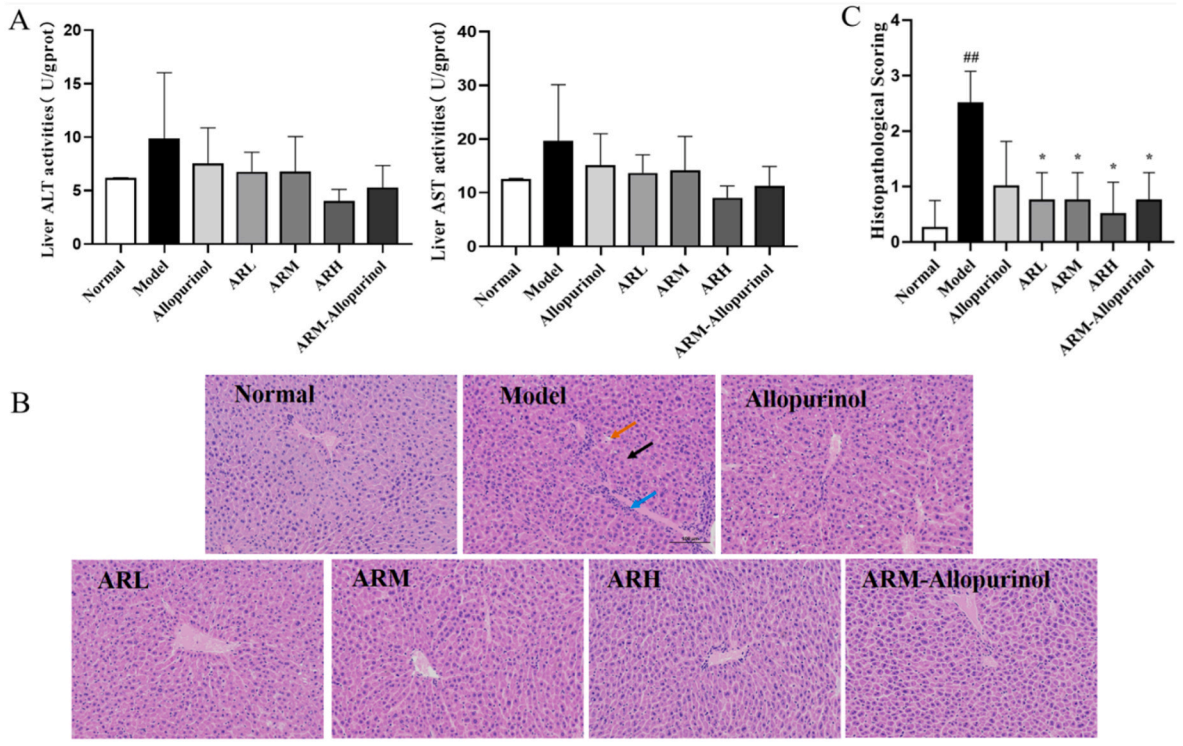


**Fig. 5.** Effects of AR on liver function in hyperuricemia mice. Note: AST and ALT activity in liver of mice (A), and pathological section of liver tissue (B). $^{\#\#}$ indicated a significantly different level from that of normal control group at $p < 0.01$; * indicated a significantly different level from that of model control group at $p < 0.05$.

When the liver is damaged, the activity value will increase significantly, thereby acting as a liver function indicator. Alanine aminotransferase (ALT) and aspartate aminotransferase (AST) are common clinical indicators to detect liver function; elevated levels of AST and ALT indicate liver damage (J. Liu et al., 2017). As shown in Fig. 5A, compared with the normal control group, the AST and ALT levels of the mice in the model control group increased slightly. Each administration group could reduce the levels of AST and ALT in mice with no significant difference compared with the model group.

Through the analysis of liver histopathological sections, no pathological changes were found in the liver tissue of the normal control group (Fig. 5B). In the model control group, a small amount of lymphocyte infiltrated in the portal canal area of the liver tissue (blue arrow), a small amount of hepatocytes around the portal vein with mild water degenerated, hepatocyte swelled, cytoplasm loosed and lightly stained (black arrow), with a small amount of mild expanded of the hepatic sinusoids (orange arrow). There was no difference between the AR treatment groups and the normal control group.

#### 3.2.5. Effect of AR on the expression of UA transporters in hyperuricemia mice

Most of the physiological UA is excreted in the urine, and only a small part is excreted in the faeces. The reabsorption and secretion of UA in the kidneys and intestines are regulated by urate transport-related proteins (Singh et al., 2011). UA enters the renal tubule after glomerular filtration and is reabsorbed into the blood by URAT1 or GLUT9 in the proximal tubule. UA is resecreted and excreted into the urine by ABCG2 (Diaz et al., 2015; Kaito et al., 2013; Ichida et al., 2012).

Western Blot results showed that AR could promote ($p < 0.001$) ABCG2 expression in a dose-dependent manner in comparison to the model control group (Fig. 6A). Especially, the high-dose AR group and ARM-allopurinol group showed significantly facilitated activities ($p < 0.001$).

As shown in Fig. 6B, compared to the normal control group, the expression of ABCG2 in kidney was decreased and the expression of URAT1 and GLUT9 was raised in model control group ($p < 0.05$). AR seems to promote ABCG2 expression, while inhibiting URAT1 and GLUT9 expression in a dose-dependent manner. This was particularly evident in the high-dose AR group and ARM-allopurinol group, which showed significant regulation activity ($p < 0.01$). These results indicated that AR could regulate the relative expression of UA transporters to reduce UA in mice.

### 3.3. Effect of AR on the expression of UA transporter in cell models

The passaged cell model derived from human organs is highly similar to human cells in terms of metabolic pathways and physiological conditions and is an important supplement to the *in vivo* mouse model. Kidneys and intestines are the main organs for uric acid excretion (Diaz et al., 2015; Kaito et al., 2013; Ichida et al., 2012). In order to further study the UA-lowering mechanism of AR, hyperuricemia CACO-2 and HK-2 cell models were used to detect the expression of UA transporters after administrated with different concentrations of AR.

#### 3.3.1. Effect of AR on the expression of UA transporter in cell models

Results indicated that the expression of ABCG2 was decreased and the expression of URAT1 and GLUT9 were increased in the model control group ($p < 0.01$) when compared with the normal control group. AR could increase ABCG2 expression in CACO-2 cell in a dose-dependent manner (Fig. 7A). Likewise, AR seems to induce ABCG2 expression in a dose-dependent manner ($p < 0.01$), while inhibiting URAT1 and GLUT9 expression in HK-2 cell (Fig. 7B). These results indicated that AR could affect the expression of UA transporters in both intestinal and renal related cells and play an important role in reducing UA.

#### 3.3.2. AR inhibit expression URAT1 and GLUT9 via regulating PI3K/Akt pathway in HK-2 cells

PI3K/Akt is a remarkable signalling pathway related to transporter expression, and UA can stimulate the expression of URAT1 and GLUT9 via PI3K/Akt signalling pathway (Zhang et al., 2021; Chen et al., 2018). To further explore the mechanism of AR, AKT inhibitor VIII (20 μM) was used in the UA-induced HK-2 cell model. In the model control group, the expression of p-AKT, URAT1 and GLUT9 was increased, but the detected levels were decreased after administration of AKT inhibitor VIII or AR (Fig. 8). This result indicated that UA may activate PI3K/Akt signalling pathway and induce physiologic hypericemia. In brief, AR could depress the UA level by regulating the UA transporters through PI3K/Akt signalling pathway.

### 3.4. The UA-lowering activity of representative components in AR

As and Ca are the main quality control components of AR in Pharmacopoeia (2020). It has been reported that As had a renoprotective effect and significantly inhibited the effects of sodium urate-induced acute gouty arthritis in rats (Xu et al., 2021; Yang et al., 2020).

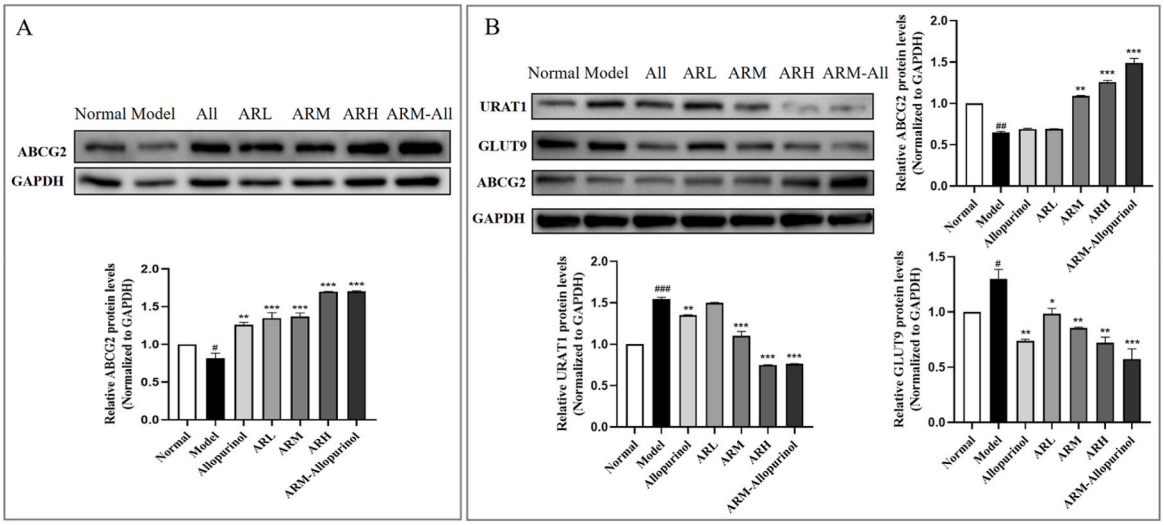


**Fig. 6.** Effects of AR on the protein expressions of UA transporters in intestine (A) and kidney (B) in hyperuricemia mice. Note: $^{\#}$, $^{\#\#}$, $^{\#\#\#}$ indicated a significantly different level from that of normal control group at $p < 0.05$, $p < 0.01$, $p < 0.001$, respectively; *, **, ***indicated a significantly different level from that of model control group at $p < 0.05$, $p < 01$, and $p < 0.001$, respectively.

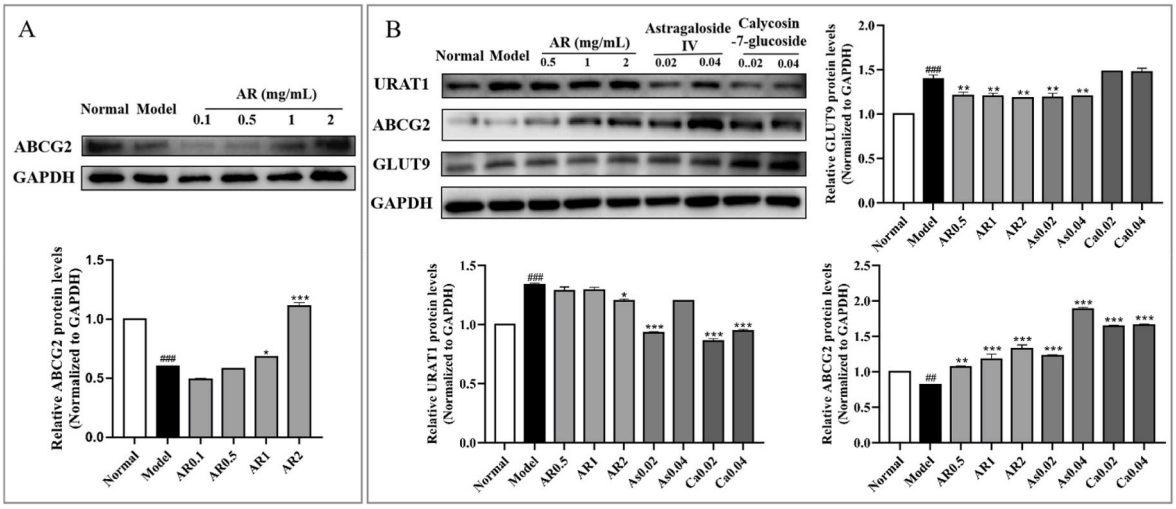


**Fig. 7.** Activity analysis of AR on UA transporters in CACO-2 (A) and HK-2 (B). Note: $^{\#\#}$, $^{\#\#\#}$ indicated a significantly different level from that of normal control group at $p < 0.01$, $p < 0.001$, respectively; *, **, *** indicated a significantly different level from that of model control group at $p < 0.05$, $p < 01$, and $p < 0.001$, respectively.

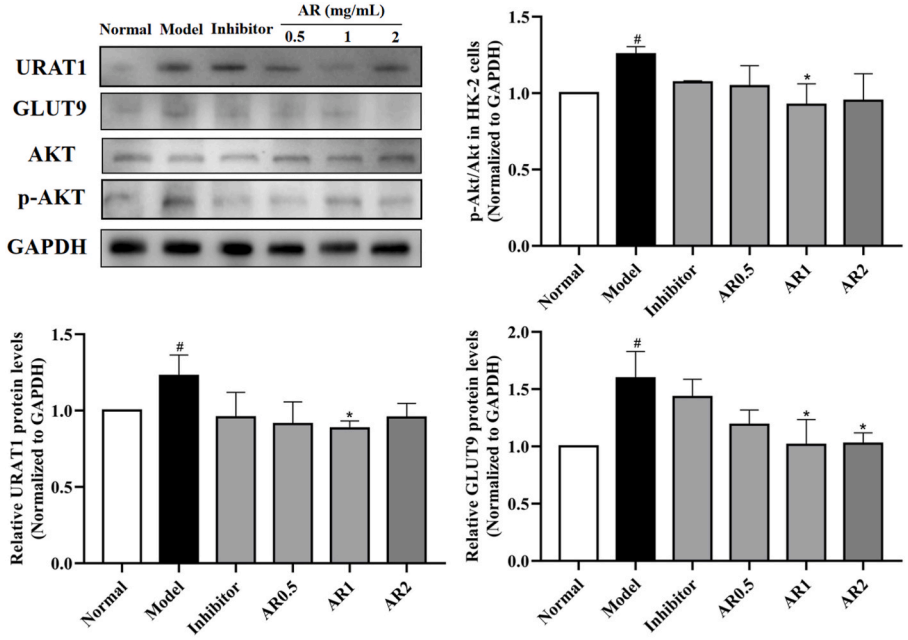


**Fig. 8.** AR inhibits expression of URAT1 and GLUT9 through repressing PI3K/Akt pathway in HK-2 cells. Note: $^{\#}$ indicated a significantly different level from that of normal control group at $p < 0.05$; * indicated a significantly different level from that of model control group at $p < 0.05$.

### *3.4.1. The expression of UA transporters in HK-2 cells*

The effects of As and Ca on the expression of UA transporters in kidney were detected in the established HK-2 hyperuricemia cell model. The results expounded that the protein expression of ABCG2 was notably increased ($p < 0.001$) when cells were treated with As and Ca, and the expression of URAT1 protein was inhibited (Fig. 7B). The same result was not observed, however, in the case of GLUT9.

### *3.4.2. Molecular docking between representative components and UA transporters*

Considering the cell experiments results, As and Ca affected the expression of UA transporters. To investigate binding patterns of ligands and UA transporters of ABCG2, GLUT9 and URAT1, the molecular docking was used. The binding patterns are shown in Fig. 9.

The binding energy of As to ABCG2 protein was −7.4 kcal/mol, and it formed 5 hydrogen bonds with amino acid residues Tyr398, Ser401, Ser444, Ile448 and Thr452 at interaction distances of 3.06 Å, 2.26 Å, 2.17 Å, 2.94 Å and 2.80 Å, respectively. The hydrophobic interactions were formed with amino acid residues Phe408 and Ile448. The binding energy of Ca to ABCG2 protein was −8.0 kcal/mol, and it formed 2 hydrogen bonds with amino acid residue Asn455 at interaction distances of 2.71 Å and 2.76 Å, respectively. The π-π interaction was formed with Tyr398 at interaction distance of 5.30 Å, and the hydrophobic interactions were formed with Tyr398, Asp395 and Ile448. The binding energy of As to GLUT9 protein was −9.8 kcal/mol, and it formed one hydrogen bond with Gly420 at an interaction distance of 2.91 Å. The hydrophobic interactions were formed with amino acid residues Pro167, Met168, Ile417 and Phe432. The binding energy of Ca to URAT1 protein was −9.1 kcal/mol, and it formed 3 hydrogen bonds with amino acid residues Glu38 (2 hydrogen bonds) and Arg487 at interaction distances

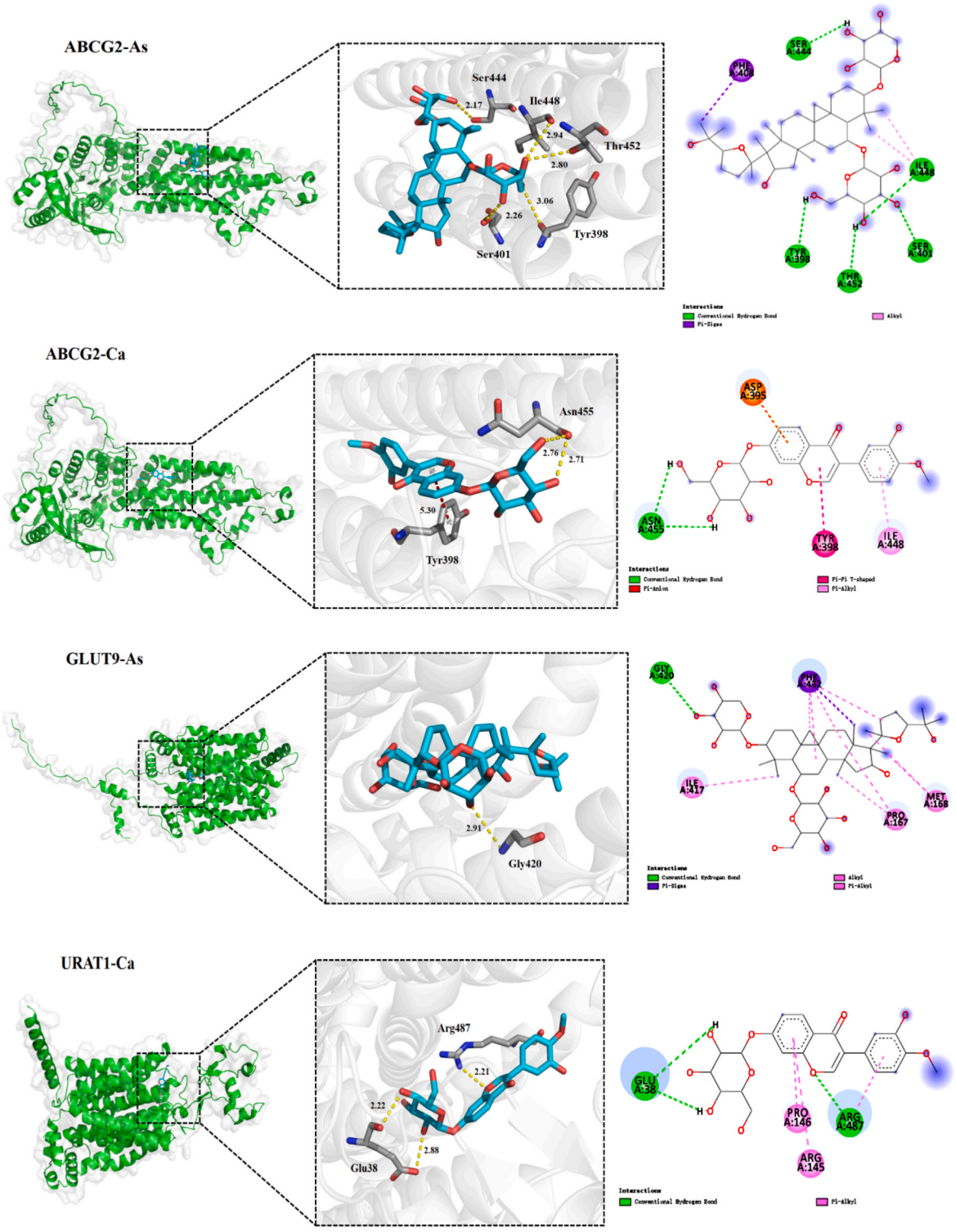


**Fig. 9.** Molecular docking study of compound As and Ca.

of 2.22 Å, 2.88 Å and 2.21 Å, respectively. The hydrophobic interactions were formed with amino acid residues Arg145 and Pro146. The docking results may provide an explanation for the prominent activity of As and Ca.

## 4. Conclusions

In this study, the UA-lowering activity and mechanism of AR were researched through the constructed hyperuricemia mouse and cellular models. The experimental results showed that the level of SUA in mice in the AR administration group was significantly decreased, and the contents of UA in urine and faeces were remarkably increased in a dose-dependent manner. The BUN, SCr levels and the activity of XOD in the liver of mice were all decreased, indicating that AR could relieve acute hyperuricemia by protecting the kidneys and reducing the production of UA. In what concerns the mechanism of action, it seems that the relative expression levels of URAT1 and GLUT9 in the AR administration group were down-regulated, and the ABCG2 was up-regulated, indicating that

AR could promote the excretion of UA by regulating UA transporters via PI3K/Akt signalling pathway. The representative components in AR also had UA-lowering activities.

Overall, AR displayed promising anti-hyperuricemia effects by regulating UA transporters, and suppressing the activity of XOD. These results offer a basis for the medicinal uses of AR on anti-hyperuricemia.

## Author contributions

Meng-Qi Zhang, Ke-Xin Sun, Cai-Yun Feng and Jia-Shu Chen gave services to the research design, data acquisition and analysis. Meng-Qi Zhang, Xu Guo, Ying-Ying Chen, Joao C.M. Barreira, Jian-Dong Zhang and Miguel A. Prieto wrote the rough draft of the article, and revised the manuscript. Chao Liu and Jin-Yue Sun were responsible for the research topic and dedicated to the research design, analysis of data, and manuscript modified. All of the authors reviewed and endorsed the final manuscript.

## Funding

This work was supported by the Central Guidance on Local Science and Technology Development Fund of Shandong, China (No. YDZX2022175; YDZX2022087); the Innovation Ability Improvement Project for Technology-Based Small and Medium-sized Enterprises of Shandong, China (No. 2022TSGC2002, 2022TSGC2065); the Provincial Major Scientific and Technological Innovation Project of Shandong, China (No. 2021SFGC0904, 2021TZXD001, 2022TZXD0029, 2022TZXD0032), the Natural Science Foundation of Shandong, China (No. ZR2020QD103; ZR2020MH401; ZR2021QH351).

## Declaration of competing interest

The authors declare that they have no known competing financial interests or personal relationships that could have appeared to influence the work reported in this paper.

## Data availability

Data will be made available on request.

## Appendix A. Supplementary data

Supplementary data to this article can be found online at https://doi.org/10.1016/j.jep.2023.116770.

## List of abbreviations

| | |
|---|---|
| AR | Astragali Radix |
| UA | uric acid |
| XOD | xanthine oxidase |
| URAT1 | uric acid transporter 1 |
| GLUT9 | glucose transporter 9 |
| ABCG2 | adenosine triphosphate transporter G2 |
| As | astragaloside IV |
| Ca | calycosin-7-glucoside |
| SDS | Sodium dodecyl sulphate |
| ALT | alanine transaminase |
| AST | aspartate transaminase |
| ARL | low-dosage AR group |
| ARM | medium-dosage AR group |
| ARH | high-dosage AR group |
| SCr | serum creatinine |
| BUN | blood urea nitrogen |
| BCA | bicinchoninic acid assay |
| PVDF | polyvinylidene fluoride |
| CACO-2 | human colon carcinoma cell line |
| HK-2 | human renal tubular epithelial cell line |
| SD | standard deviation |
| SUA | serum UA |
| UUA | UA in urine |
| FUA | UA in faeces |

## References

Bian, Y.Y., Li, P., 2008. Studies on chemical constituents of Astragalus membranaceus (Fisch.) B. ge. var. mongholicus (Bge.) Hsiao. J. Chin. Pharm. 41 (16), 1217–1221.
Bin, G., Gao, Y., Liang, J., He, J., Liu, Y., Wang, W., 2020. Application of Astragalus in Chinese medicine surgery. Chin. J. Surg. Integr. Tradit. Western Med. 26 (6), 1202–1205.
Chen, J.S., Wang, M.X., Wang, M.M., Zhang, Y.K., Guo, X., Chen, Y.Y., Zhang, M.Q., Sun, J.Y., Liu, Y.F., Liu, C., 2022. Synthesis and biological evaluation of geniposide derivatives as inhibitors of hyperuricemia, inflammatory and fibrosis. Eur. J. Med. Chem. 237, 114379.
Chen, M., Lu, X.Y., Lu, C., Shen, N., Jiang, Y.J., Chen, M.L., Wu, H.X., 2018. Soluble uric acid increases PDZK1 and ABCG2 expression in human intestinal cell lines via the TLR4-NLRP3 inflammasome and PI3K/Akt signaling pathway. Arthritis Res. Ther. 1, 20.
Chinese Pharmacopoeia Commission, 2020. Pharmacopoeia of People's Republic of China. Medical Science Press of China, Beijing, China.
Dalbeth, N., Phipps-Green, A., Frampton, C., 2018. Relationship between serum urate concentration and clinically evident incident gout: an individual participant data analysis. Ann. Rheum. Dis. 77 (7), 212288 annrheumdis-2017.
Diaz, T., Cesar, P.H.N., Perez-Ruiz, F., 2015. New medications in development for the treatment of hyperuricemia of gout. Curr. Opin. Rheumatol. 27 (2), 164–169.
Fukunari, A., Okamoto, K., Nishino, T., Eger, B.T., Pai, E.F., Kamezawa, M., Yamada, I., Kato, N., 2004. Y-700 [1-[3-Cyano-4-(2, 2-dimethylpropoxy) phenyl]-1H-pyrazole-4-carboxylic acid]: a potent xanthine oxidoreductase inhibitor with hepatic excretion. J. Pharmacol. Exp. Therapeut. 311, 519–528.
Han, S., Wei, R., Han, D., 2020. Hypouricemic Effects of extracts from urtica hyperborea Jacq. ex Wedd. in hyperuricemia mice through XOD, URAT1, and OAT1. BioMed Res. Int. 11, 1–8.
Hille, R., 2006. Structure and function of xanthine oxidoreductase. Eur. J. Inorg. Chem. 10, 1913–1926.
Hong, H., Wen, J., Chen, Z., 2016. The research progress on pharmacological effects of Astragalus membranaceus. World Latest Med. Inform. 16 (14), 49–50, 69.
Ichida, K., Matsuo, H., Takada, T., 2012. Decreased extra-renal urate excretion is a common cause of hyperuricemia. Nat. Commun. 3, 764.
Jin, M.L., Zhao, K., Huang, Q., Shang, P., 2014. Structural features and biological activities of the polysaccharides from Astragalus membranaceus. Int. J. Biol. Macromol. 64, 257–266.
Kaito, H., Ishimori, S., Nozu, K., 2013. Molecular background of urate transporter genes in patients with exercise-induced acute kidney injury. Am. J. Nephrol. 38 (4), 316–320.
Lin, H., Tu, C., Niu, Y., 2019. Dual actions of norathyriol as a new candidate hypouricaemic agent: uricosuric effects and xanthine oxidase inhibition. Eur. J. Pharmacol. 853, 371–380.
Liu, C.H., Yen, M.H., Tsang, S.F., Gan, K.H., Hsu, H.Y., Lin, C.N., 2010. Antioxidant triterpenoids from the stems of Momordica charantia. Food Chem. 118 (3), 751–756.
Liu, H., Li, Z., Zhang, P., 2017. Clinical observation of Huangqi Baoxin Decotion on chronic heart failure complicated with hyperuricemia. J. Emerg. Tradit. Chin. Med. 26 (9), 1651–1654.
Liu, J., Fu, Y., Zhang, H., Wang, J.D., Zhu, J., Wang, Y.Q., Guo, Y.G., Wang, G.C., Xu, T. Q., Chu, M.P., Wang, F.Y., 2017. The hepatoprotective effect of the probiotic *Clostridium butyricum* against carbon tetrachloride-induced acute liver damage in mice. Food Funct. 8, 4042–4052.
Liu, J., Li, L., 2010. Athogenesy and pharmacotherapy of hyperuricemia: research advances. J. Int. Pharmacol. Res. 37 (1), 24–28.
Mann, P., 2019. In: Yang, L.F., Zhou, X.M., Zhao, D.M. (Eds.), International Harmonization of Nomenclature and Diagnostic Criteria for Lesions in Rats and Mice (INHAND). China Agricultural Press, Beijing (translated).
Singh, J.A., Reddy, S.G., Kundukulam, J., 2011. Risk factors for gout and prevention: a systematic review of the literature. Curr. Opin. Rheumatol. 23 (2), 192–202.
Song, X., Lei, Y., Liu, N., Hu, J., Sun, L., Li, S., 2021. Research advances in regulation and mechanism of active substances from food and medicine resources on uric acid metabolism. Acta Agric. Boreali-Sinice 36 (S1), 188–194.
Syahrina, Asfianti, V., Gurning, K., Iksen, 2020. Phytochemical screening and anti-hyperuricemia activity test in vivo of ethanolic extract of shallot (*Allium cepa* L.) skin. Borneo J. Pharm. 3 (3), 146–151.
Tang, F., Zhang, Q., Nie, Z., Yao, S., Chen, B., 2009. Sample preparation for analyzing traditional Chinese medicines. Trends Anal. Chem. 28 (11), 1253–1262.
Umekawa, T., Chegini, N., Khan, S.R., 2003. Increased expression of monocyte chemoattractant protein-1 (MCP-1) by renal epithelial cells in culture on exposure to calcium oxalate, phosphate and uric acid crystals. Nephrol. Dial. Transplant. 18, 664–669.
Wang, C.P., Wang, Y., Wang, X., 2010. Mulberroside a possesses potent uricosuric and nephroprotective effects in hyperuricemic mice. Planta Med. 77 (8), 786–794.
Wang, H., Liu, N., Li, Y., Zou, J., Zhang, S., Zhang, X., 2021. Comparative study on effects of 5 kinds of Chinese herbs produced in Gansu province on gout. Chin. J. Tradit. Med. Sci. Technol. 28 (5), 720–722.

Wang, J.S., 2016. To explore the application value of HE staining method in clinicopathological diagnosis. World Latest Med. Inform 16 (68), 144–149.
Wang, X., Xue, N., Li, H., Chen, Z., Yu, W., 2020. Study on mechanism of Fangji Huangqi Decoction on hypouricemic effect and renal protection in hyperuricemia mice. China J. Chin. Mater. Med. 45 (21), 5248–5255.
Xu, Y., Ding, Y., Liu, S., Kang, J., Shao, B., 2021. Protective effect of astragaloside on renal injury induced by radiation through toll-like receptor 4/nuclear factor kappa B pathway. Acta Anat. Sin. 52 (4), 621–627.
Xu, Z., Dai, X., Zhang, Q., Su, S., Yan, H., Zhu, Y., Shang, E., Qian, D., Duan, J., 2020. Protective effects and mechanisms of Rehmannia glutinosa leaves total glycoside on early kidney injury in db/db mice. Biomed. Pharmacother. 125, 109926.
Yan, M.M., Liu, W., Fu, Y.J., Zu, Y.G., Chen, C.Y., Luo, M., 2010. Optimisation of the microwave-assisted extraction process for four main astragalosides in Radix Astragali. Food Chem. 119, 1663–1670.
Yang, D., Shan, Y., Zhang, X., Wang, L., 2020. Preventive and therapeutic effects of astragaloside IV on acute gouty arthritis induced by sodium urate in rats and the mechanism of inflammation. Heb. Med. J. 42 (15), 2245–2249.
Yong, T., Chen, S., Xie, Y., 2018. Hypouricemic effects of extracts from Agrocybe aegerita on hyperuricemia mice and virtual prediction of bioactives by molecular docking. Front. Pharmacol. 9, 498.
Yuan, L.A., Sheng, G.A., Yue, Z.A., 2019. Comparative analysis of twenty-five compounds in different parts of Astragalus membranaceus var. mongholicus and Astragalus membranaceus by UPLC-MS/MS. J. Pharm. Anal. 9 (6), 392–399.
Zeng, N., Zhang, G., Hu, X., 2019. Mechanism of fisetin suppressing superoxide anion and xanthine oxidase activity. J. Funct.Foods 58, 1–10.
Zhang, B.Q., Hu, S.J., Qiu, L.H., Zhu, J.H., Xie, X.J., Sun, J., 2007. Effects of Astragalus membranaceus and its main components on the acute phase endothelial dysfunction induced by homocysteine. Vasc. Pharmacol. 46, 278–285.
Zhang, M.Q., Ren, X., Zhao, Q., Yue, S.J., Fu, X.M., Li, X., Chen, K.X., Guo, Y.W., Shao, C. L., Wang, C.Y., 2020. Hepatoprotective effects of total phenylethanoid glycosides from *Acanthus ilicifolius* L. against carbon tetrachloride-induced hepatotoxicity. J. Ethnopharmacol. 256, 112795.
Zhang, Y., Tan, X.H., Lin, Z., Li, F.P., Yang, C.Y., Zheng, H.Y., Li, L.Y., Liu, H.Z., Shang, J. H., 2021. Fucoidan from laminaria japonica inhibits expression of GLUT9 and URAT1 via PI3K/Akt, JNK and NF-κB pathways in uric acid-exposed HK-2 cells. Mar. Drugs 5, 238.
Zhang, Z., Li, T., Zhang, M., 2018. The treatment of gout from the spleen and kidney by Yuqi Dang. Shanxi J. Tradit. Chin. Med. 34 (10), 3.
Zheng, Y., Ren, W., Zhang, L., Zhang, Y., Liu, D., 2020. A review of the pharmacological action of Astragalus Polysaccharide. Front. Pharmacol. 11, 349.
Zhou, H., Chen, Y., 2014. Anti-hyperuricemic activity of bergenin and its mechanism. Acta Univ. Med. Anhui 49 (1), 63–67.